Archives of Microbiology
https://doi.org/10.1007/s00203-020-02057-w

SHORT COMMUNICATION

Genomic and phenotypic analysis of siderophore-producing *Rhodococcus qingshengii* strain S10 isolated from an arid weathered serpentine rock environment

Irina V. Khilyas[1] · Alyona V. Sorokina[1] · Maria I. Markelova[1] · Maksim Belenikin[2] · Lilia Shafigullina[1] · Rezeda I. Tukhbatova[3] · Elena I. Shagimardanova[4] · Jochen Blom[5] · Margarita R. Sharipova[1] · Michael F. Cohen[6]

Received: 13 April 2020 / Revised: 8 July 2020 / Accepted: 17 September 2020

Abstract

The success of members of the genus *Rhodococcus* in colonizing arid rocky environments is owed in part to desiccation tolerance and an ability to extract iron through the secretion and uptake of siderophores. Here, we report a comprehensive genomic and taxonomic analysis of *Rhodococcus qingshengii* strain S10 isolated from eathered serpentine rock at the arid Khalilovsky massif, Russia. Sequence comparisons of whole genomes and of selected marker genes clearly showed strain S10 to belong to the *R. qingshengii* species. Four prophage sequences within the *R. qingshengii* S10 genome were identified, one of which encodes for a putative siderophore-interacting protein. Among the ten non-ribosomal peptides synthase (NRPS) clusters identified in the strain S10 genome, two show high homology to those responsible for siderophore synthesis. Phenotypic analyses demonstrated that *R. qingshengii* S10 secretes siderophores and possesses adaptive features (tolerance of up to 8% NaCl and pH 9) that should enable survival in its native habitat within dry serpentine rock.

Keywords *Rhodococcus qingshengii* · Desiccation · Siderophores · Serpentinite · Phenotype · Pan-genome

Members of the genus *Rhodococcus* (phylum *Actinobacteria,* family *Nocardiaceae*) can degrade and transform a range of environmental pollutants or synthesize compounds with commercially useful applications (Christofi and Ivshina 2002). Over the past 20 years, rhodococci have found predominant use as a bioremediation and bioconversion tool with relatively little attention given to their potential for biosynthesis of natural products for use in the pharmaceutical and agricultural sectors (Ceniceros et al. 2017).

Along the spectrum of rhodococcal metabolites, there are several hydroxamate- and catecholate-type siderophores, including heterobactins, rhodobactin, rhodochelin, rhequichelin and rhequibactin (Bosello et al. 2011, 2013; Carrano et al. 2001; Dhungana et al. 2007; Miranda-CasoLuengo et al. 2008). Siderophores also find numerous applications in ecology (increasing iron availability to soil microorganisms), agriculture (biological control of plant pathogens and plant growth promotion), bioremediation (detoxifying heavy metal contaminated sites), and medicine (regulation of oxidative stress, providing of antibacterial activity, mediating delivery of antibiotics to antibiotic resistant bacteria, treatment of iron overload diseases, antimalarial activity, and cancer therapy) (Johnstone and Nolan 2015; Saha et al. 2016).

Communicated by Erko Stackebrandt.

✉ Irina V. Khilyas
irina.khilyas@gmail.com

[1] Department of Microbiology, Institute of Fundamental Medicine and Biology, Kazan (Volga Region), Federal University, Kazan, Russian Federation

[2] Department of Molecular and Biological Physics, Moscow Institute of Physics and Technology (State University), Dolgoprudny, Russia

[3] Laboratory of Structural Biology, Institute of Fundamental Medicine and Biology, Kazan (Volga Region), Federal University, Kazan, Russian Federation

[4] Laboratory of Extreme Biology, Institute of Fundamental Medicine and Biology, Kazan (Volga Region), Federal University, Kazan, Russian Federation

[5] Bioinformatics and Systems Biology, Justus-Liebig-University Giessen, Giessen, Germany

[6] Department of Biology, Sonoma State University, Rohnert Park, CA, USA

Published online: 06 October 2020

Rhodococci are ubiquitous members of microbial communities in different terrestrial ecosystems with different water availability (Alvarez 2019). Arid rocky environments present harsh living conditions for bacteria, with extreme fluctuations of pH, temperature, moisture and nutrient availability (Gadd 2010). Mechanisms of bacterial acclimation to extremely low water content include up-regulation of genes responsible for the synthesis of proteins participating in oxidative stress responses and protein stabilization and increasing production of extracellular polysaccharides and concentrations of intracellular solutes (Potts 1994). For instance, the desiccation-tolerant *Rhodococcus jostii* strain RHA1 responds to drying by upregulating transcription of the genes encoding the oxidative stress protection protein dps1, two sigma factors, and the biosynthetic pathway for the compatible solute ecotine (LeBlanc et al. 2008).

We previously characterized the geochemistry and microbial communities of latitudinal samples from a core of weathered serpentine rock drilled at the Khalilovsky massif, Russia (Latitude: N 51°30′ Longitude: E 58° 11′) (Khilyas et al. 2019). Strain S10 was isolated from a colony on Luria Agar (LA) agar that had been plated with aqueous rinsate of crushed rock taken from the 10-cm core depth. Cells of strain S10 were rod-shaped (0.6–0.7 µm wide, 2–5 µm long; Fig. S1), Gram-positive, non-sporulating and non-motile and formed small (0.5–1.0 mm), round and semitransparent colonies with a smooth shape and glistening surface after 24 h of cultivation on LA at 30 °C.

Genomic DNA from strain S10 was extracted from an overnight LB-grown culture using the Fast DNA™ SPIN Kit (*MP Biomedicals, USA*). A paired-end DNA library was prepared using the TruSeq DNA HT Library Preparation kit (Illumina) according to manufacturer guidelines. Whole-genome sequencing was carried out by Miseq sequencing platform (Illumina) with 250 bp read length and the quality of the raw sequence reads was evaluated by FastQC package (v0.11.3) (Andrews 2010). The genome had an average 246X sequencing coverage. Overrepresented and low-quality sequences were removed using Trimmomatic (v0.36) (Bolger et al. 2014). The whole genome was assembled using Ray (v2.3.1) software with different k-mer sizes (Pevzner et al. 2001). The k-mer-based correctness is counted in the QUAST (v4.6.2) program (Gurevich et al. 2013). Genome annotation was performed by Rapid Annotation using Subsystem Technology (RAST 2.0) server, Prokka (v1.13) annotation pipeline and the NCBI Prokaryotic Genomes Annotation Pipeline (PGAP) version 4.8 (Aziz et al. 2008; Tatusova et al. 2016). The PGAP and RAST annotations resulted in minor differences (Table S1). The genome coding density was 90.6% (completeness 99.9% and contamination 0.31%) with an average gene length of 945.9 bp. The size of the assembled near-complete genome of strain S10 was 7,184,029 bp, comprising 64 contigs, with a G + C content of 62.4%. Strain S10 contained 6,834 predicted genes, 6,564 putative coding sequences (CDS), 16 rRNAs, 53 tRNAs and 3 ncRNAs. The RAST annotation of the strain S10 genome revealed 7069 coding regions, among them 2330 (33%) functionally annotated (Fig. S3). The genome contains 154 genes involved in stress responses and 21 genes in iron acquisition and metabolism (Fig. S3).

Pairwise sequence similarities calculated using 16S rRNA genes available via the GGDC web server (https://ggdc.dsmz.de/) showed that strain S10 clusters with the *R. qingshengii* species group (Fig. S2).

To better establish the taxonomic position of strain S10 and assess its genome-encoded and expressed physiologic capabilities, we conducted a variety of in situ genome sequence comparisons as well as phenotypic tests. The Average Nucleotide Identity (ANI) of the strain S10 genome was analyzed using EDGAR (Blom et al. 2016). ANI values ≥ 97.98% were obtained with genomes assigned to *R. qingshengii* (Fig. S4). In silico DNA–DNA hybridization (DDH) comparisons with GGDC2.0 (Meier-Kolthoff et al. 2013) between the genome of strain S10 and other accessible *Rhodococcus* genome sequences in GenBank indicated the closest match to *Rhodococcus jialingiae* djl-6–2 (a homotypic synonym of *Rhodococcus qingshengii*) with an estimated DDH value (high-scoring segment pair length/total length, generalized linear model-based) of 81.6% and to the *R. qingshengii* type strain (JCM 15477) with an estimated DDH value of 74.6% (Fig. S5). Comparative genomic analysis of coding sequence regions (CDSs) in *R. qingshengii* strains, performed using a web server for the analysis of large-scale microbial genomics data (https://microbializer.tau.ac.il), revealed 6889 orthologous CDSs (Avram et al. 2019). It was found that 95.5% and 94.6% of the ORFs in the S10 genome have homologs in the genomes of *R. qingshengii* RL1 and *R. qingshengii* BKS 20–40, respectively (Table S2).

MultiLocus Sequence Analysis (MLSA) of strain S10, based on conserved marker genes (*ftsY, infB, rpoB, rsmA, secY, tsaD*, and *ychF*) within the subclass *Actinobacteridae* (Creason et al. 2014), was performed using the Gall-ID platform (Stamatakis 2014). The resulting phylogenetic tree, based on sequence alignments with *R. erythropolis* PR4 as a reference strain, was consistent with the tree generated from whole-genome alignments (Fig. S6). Gyrase B (*gyr*B) and catechol 1,2-dioxygenase (*cat*A) gene sequence comparisons, in conjunction with DDH analysis, have been applied to establish species identity of *R. quingshengii* strains (Tancsics et al. 2014). The *gyr*B and catechol 1,2-dioxygenase *cat*A of strain S10 share 99.09% and 99.81% gene homology, respectively, with the homologs in the type strain of *R. qingshengii* (DSM 4522). Thus, all of the many genetic sequence comparison methods we applied consistently

indicated strain S10 to be an isolate of *Rhodococcus qingshengii*.

A core genome-based phylogeny was created using the EDGAR platform. The core genome of 17 genomes was calculated, resulting in 2958 core genes per genome (50,826 CDS in total) with 920,028 amino acid residues per genome (15,640,476 in total). The core gene sets were aligned using the MUSCLE software (Edgar 2004). The resulting alignments were concatenated and used as input for the FastTree 2.1 approximate maximum likelihood method (Price et al. 2010). The generated tree topology, verified using the built-in Shimodaira-Hasegawa (SH) test (Shimodaira and Hasegawa 1999), showed strain S10 to fall within the monophyletic *R. qingshengii* cluster (Fig. 1). Pan-genome analysis of the 9 *R. qingshengii* genomes was carried out using Roary (Fig. S7) (Page et al. 2015). A total of 13,564 gene clusters were found: 4925 core genes (36.3%), 6467 accessory genes (cloud; 47.7%) and 2172 genes found in two or more genomes (shell; 16.0%) (Fig. S7A). The total number of genes in the pan-genome does not reach a plateau after adding a number of genomes of *R. qingshengii* strains (Fig. S7B). Thus, *R. qingshengii* strains have an open pan-genome with high genomic plasticity within this species (Sitto and Battistuzzi 2019). To visualize the differences between genomes, a presence–absence matrix was created (Fig. S7C). The unique gene clusters found for the *R. qingshengii* S10 are highlighted. Among 1116 unique genes in the *R. qingshengii* S10 genome, three Universal stress proteins, General stress protein 16U, and two putative siderophore-binding lipoproteins YfiY were found (Table S6). The strain-specific genomic difference of pan-genome of *R. qingshengii* strains was analyzed using eggNOG-mapper v2 (Fig. S7D) (Huerta-Cepas et al. 2017). Annotation for 10,800 protein sequences was performed. A significant fraction of the proteins is associated with transcription (K; 1102 genes), amino acid transport and metabolism (E; 973 genes), lipid transport and metabolism (I; 833 genes), replication, recombination and repair (L; 816 genes), and inorganic transport and metabolism (P; 741 genes).

The *PHAge* Search Tool (PHAST) web server was used to identify prophage sequences within the *R. qingshengii* strain S10 genome (Zhou et al. 2011). Four *prophage-like regions* containing 8–10 CDSs with the average size 41.7 kb were found. One of the regions includes non-phage like protein (siderophore-interacting protein) (highlighted blue in Table S3). Prophages contribute to genetic diversity of bacterial genomes and increase a fitness effect on chromosome organization.

Twenty biosynthetic gene clusters were predicted to be present in the genome of strain S10 by the antiSMASH software (Blin et al. 2019). Among those, two putative polyketide synthases (PKSs) and ten putative NRPSs gene clusters were identified. Two NRPS clusters have high sequence homology to clusters known to encode for siderophore production. One cluster has 100% similarity to the heterobactin gene cluster found in *R. qingshengii* BKS 20–40, *Rhodococcus* sp. ADH, and *R. erythropolis* SK121, while the second cluster has 57% similarity to the erythrochelin gene cluster of *R. qingshengii* BKS 20–40 and *R. erythropolis* CCM2595. We also showed that *R. qingshengii* S10 can produce siderophores in chrome azurol S (CAS) agar and in liquid M9 medium under iron-limiting conditions (Fig. 2) using the methods of Arnow (1937).

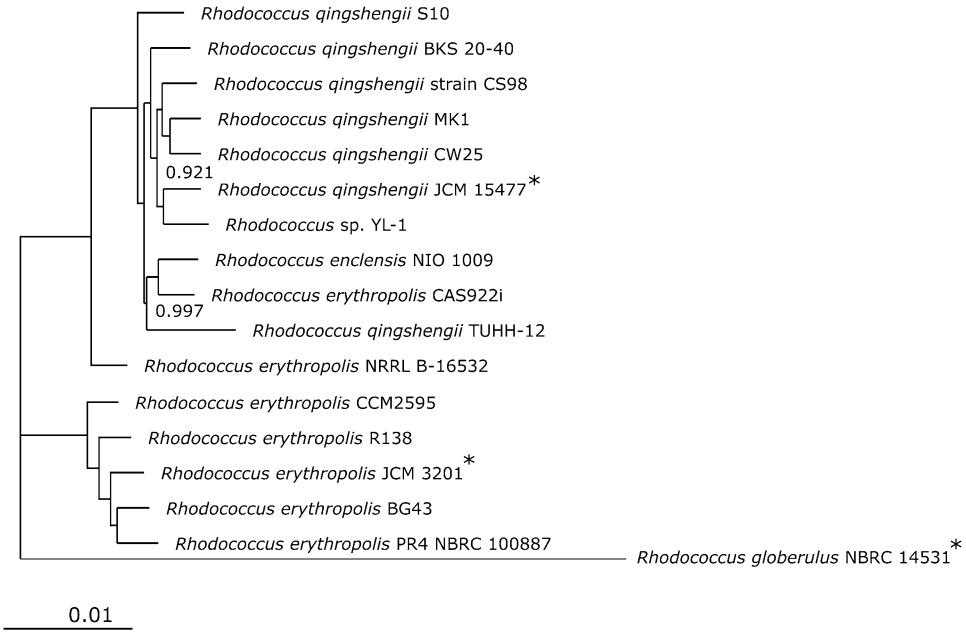

Fig. 1 Core-genome-based phylogenetic tree of 17 *Rhodococcus* genomes. The core gene sets were aligned using the MUSCLE software. A maximum-likelihood phylogenetic tree was built using FastTree 2.1 as implemented in the EDGAR platform. The final alignment included the amino acid sequences of 2958 core genes per genome present in the core-genome of the selected bacteria, 50,286 in total. Conservation values are shown at the branches. Branches without values have a perfect SH score of 1.000. Asterisks indicate type strains. *Rhodococcus enclensis* is a homotypic synonym of *Rhodococcus qingshengii* (Sangal et al. 2019)

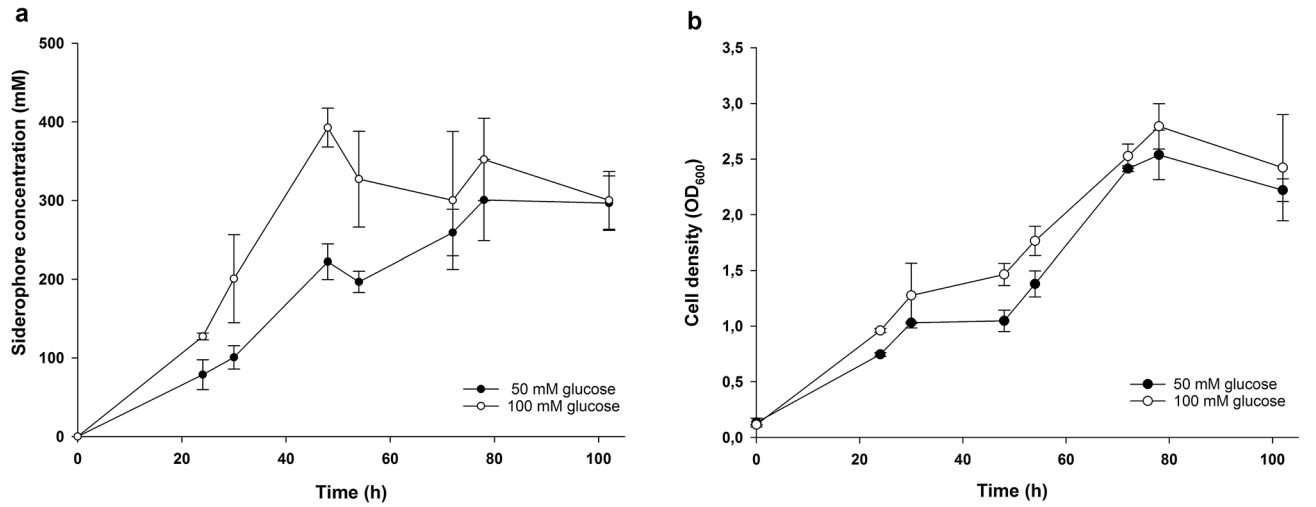

Fig. 2 Production of catecholate siderophores (**a**) and growth of *R. qingshengii* S10 (**b**) under iron-limited conditions. Error bars represent the standard deviation of duplicate experiments

Cells of strain S10 were inoculated into Biolog GEN III microplates to test for consumption of carbon sources, polymers, and amino acids, sensitivity to antibiotics and antiseptics, and growth under different pHs and salt concentrations (Bochner et al. 2001). Among all *GEN III* microplate tested substrates, *R. gingshengii* S10 was metabolically inactive only in the presence of polymers (dextrin, gelatin and pectin), D-sorbitol, p-hydroxy-phenylacetic acid, γ-aminobutyrate, α-hydroxybutyrate, D-maltose, D-raffinose (Table S4). Antibiotic resistance was found only to the monobactam aztreonam. Cells grew in the presence of NaCl at up to 8% and at a pH range of 5–9. Cells were negative for oxidase, gelatin liquefaction, and nitrate reduction, while positive for catalase and urease production. No hemolytic activity was observed on Columbia agar with 5% sheep blood (Bio-Rad) and cells did not form colonies on standard bile-esculin agar (BD Biosciences). Results of biochemical tests comparing *R. qingshengii* S10 with other strains in the *R. qingshengii–R. degradans* species group are presented in Table 1.

The presence of osmostress-responsive genes in the genome of *R. gingshengii* S10 may indicate physiological adaptation to desiccation or hypersaline conditions. The *ect*ABC genes of the pathway for ectoine biosynthesis (NCBI protein accession numbers THJ71464, THJ71463, THJ71462, respectively) are located close together in the genome S10 but are distant from the *ect*D gene (THJ65743), which encodes for an enzyme that hydroxylates ectoine to hydroxyectoine. Another solute involved in tolerance to high salinity, temperature fluctuations and desiccation stress is trehalose (Leon et al. 2018). Twelve genes from biosynthetic pathways involved in trehalose synthesis were identified in the *R. gingshengii* S10 genome and a trehalose pathway map was reconstructed using the Kyoto Encyclopedia of Genes

Table 1 Comparative characteristics of selected strains within the *R. qingshengii–R. degradans* species group

Characteristic	*R. qingshengii* S10	*R. qingshengii* sp. nov. djl-6 ^{T}	*R. erythropolis* M1	*R. degradans* strain CCM 4446 ^{T}
Gelatin liquefaction	–	ND	–	–
Dextrin	–	+	ND	ND
Tween 40/80	+/+	+/+	ND/+	+/+
Urea hydrolysis	+	+	–	–
Nitrate reduction	–	–	+	–
Oxidase	–	–	–	–
Catalase	+	+	+	+
Reference	This study	Xu et al. 2007	Goswami et al. 2005	Švec et al. 2015

+positive; – negative; *w* weakly positive; *ND* not determined

and Genomes (KEGG) mapping tool (Fig. S8, Table S5) (Kanehisa and Goto 2000).

BLAST comparison of the desiccation tolerance-related *dps*1 gene sequence (Non-specific DNA-binding protein Dps/Iron-binding ferritin-like antioxidant protein/Ferroxidase; NCBI gene accession number WP_003943731) of *R. qingshengii* S10 revealed 78.83% identity with the *dps*1 of *R. jostii* RHA1 (NCBI gene accession number 4224921) (LeBlanc et al. 2008).

Hydrophobicity of the *R. gingshengii* S10 cell surface was measured by the salt aggregation test (SAT), which is based on the ability of bacterial cells to form autoaggregates in ammonium sulfate solutions of various molarities (0.02–4.0, pH 6.8) (Ljungh et al. 1985). *R. quingshengii* S10 aggregated in the range of 0.1–0.4 M ammonium sulfate, indicating a high surface hydrophobicity that confers an ability to migrate to the hydrophobic layer in organic-aqueous systems.

R. gingshengii S10 was deposited under the strain accession number Ac-2085 in the Russian National Collection of Industrial Microorganisms (VKPM).

Nucleotide sequence accession number This whole-genome shotgun project has been deposited at DDBJ/ENA/GenBank under the accession NZ_SSWN00000000.1.

The comprehensive genomic analysis identified bacterial strain 10, isolated from arid ultramafic rock, as *Rhodococcus qingshengii*. Strain S10 has characteristics associated with adaptation to desiccation, including tolerance to high NaCl levels, growth at alkaline pH, high cell wall hydrophobicity, the presence of genes for biosynthesis of ectoine and trehalose, and the *dps1* gene. Moreover, the excretion of siderophores, demonstrated by the presence of biosynthetic gene clusters responsible for their synthesis and their accumulation in culture, provides cells means to extract metals from their mineral substrate.

Acknowledgements This work was supported by the Russian Science Foundation (grant No 19-74-00062) and performed in accordance with the Program of Competitive Growth of Kazan Federal University. The authors are grateful to the Interdisciplinary Center for Collective Use (ID RFMEFI59414X0003) sponsored by the Ministry of Education and Science of the Russian Federation. Microscopy studies were carried out at the Interdisciplinary Center of Analytical Microscopy of Kazan Federal University.

References

Alvarez HM (2019) Biology of *Rhodococcus*. In: Alvarez H (ed) Biology of *Rhodococcus.* Microbiology Monographs 16. Springer, Nature Switzerland AG

Andrews S (2010) FastQC: a quality control tool for high throughput sequence data. http://www.bioinformatics.babraham.ac.uk/projects/fastqc/. Accessed 2010

Arnow E (1937) Colorimetric determination of the components of 3,4-dihydroxyphenylalanine-tyrosine mixtures. J Biol Chem 118:531–537

Avram O, Rapoport D, Portugez S, Pupko T (2019) M1CR0B1AL1Z3R—a user-friendly web server for the analysis of large-scale microbial genomics data. Nucleic Acids Res 47:W88–W92

Aziz RK, Bartels D, Best AA et al (2008) The RAST server: rapid annotations using subsystems technology. BMC Genomics 9:75. https://doi.org/10.1186/1471-2164-9-75

Blin K et al (2019) antiSMASH 5.0: updates to the secondary metabolite genome mining pipeline. Nucleic Acids Res 47:W81–W87. https://doi.org/10.1093/nar/gkz310

Blom J, Kreis J, Spanig S, Juhre T, Bertelli C, Ernst C, Goesmann A (2016) EDGAR 2.0: an enhanced software platform for comparative gene content analyses. Nucleic Acids Res 44:W22–28. https://doi.org/10.1093/nar/gkw255

Bochner BR, Gadzinski P, Panomitros E (2001) Phenotype microarrays for high-throughput phenotypic testing and assay of gene function. Genome Res 11:1246–1255. https://doi.org/10.1101/gr.186501

Bolger AM, Lohse M, Usadel B (2014) Trimmomatic: a flexible trimmer for Illumina sequence data. Bioinformatics (Oxford, England) 30:2114–2120. https://doi.org/10.1093/bioinformatics/btu170

Bosello M, Robbel L, Linne U, Xie X, Marahiel MA (2011) Biosynthesis of the siderophore rhodochelin requires the coordinated expression of three independent gene clusters in *Rhodococcus jostii* RHA1. J Am Chem Soc 133:4587–4595. https://doi.org/10.1021/ja1109453

Bosello M, Zeyadi M, Kraas FI, Linne U, Xie X, Marahiel MA (2013) Structural characterization of the heterobactin siderophores from *Rhodococcus erythropolis* PR4 and elucidation of their biosynthetic machinery. J Nat Prod 76:2282–2290. https://doi.org/10.1021/np4006579

Carrano CJ, Jordan M, Drechsel H, Schmid DG, Winkelmann G (2001) Heterobactins: A new class of siderophores from *Rhodococcus erythropolis* IGTS8 containing both hydroxamate and catecholate donor groups. Biometals 14:119–125. https://doi.org/10.1023/a:1016633529461

Ceniceros A, Dijkhuizen L, Petrusma M, Medema MH (2017) Genome-based exploration of the specialized metabolic capacities of the genus *Rhodococcus*. BMC genomics 18:593. https://doi.org/10.1186/s12864-017-3966-1

Christofi N, Ivshina IB (2002) Microbial surfactants and their use in field studies of soil remediation. J Appl Microbiol 93:915–929. https://doi.org/10.1046/j.1365-2672.2002.01774.x

Creason AL, Davis EW 2nd, Putnam ML, Vandeputte OM, Chang JH (2014) Use of whole genome sequences to develop a molecular phylogenetic framework for Rhodococcus fascians and the *Rhodococcus* genus Front. Plant Sci 5:406. https://doi.org/10.3389/fpls.2014.00406

Dhungana S et al (2007) Purification and characterization of rhodobactin: a mixed ligand siderophore from *Rhodococcus rhodochrous* strain OFS. Biometals 20:853–867. https://doi.org/10.1007/s10534-006-9079-y

Edgar RC (2004) MUSCLE: multiple sequence alignment with high accuracy and high throughput. Nucleic Acids Res 32:1792–1797. https://doi.org/10.1093/nar/gkh340

Gadd GM (2010) Metals, minerals and microbes: geomicrobiology and bioremediation microbiology. Geomicrobiol Bioremed Microbiol (Reading, England) 156:609–643. https://doi.org/10.1099/mic.0.037143-0

Goswami M, Shivaraman N, Singh RP (2005) Microbial metabolism of 2-chlorophenol, phenol and rho-cresol by *Rhodococcus erythropolis* M1 in co-culture with *Pseudomonas fluorescens* P1. Microbiol Res 160:101–109. https://doi.org/10.1016/j.micres.2004.10.004

Gurevich A, Saveliev V, Vyahhi N, Tesler G (2013) QUAST: quality assessment tool for genome assemblies. Bioinformatics (Oxford, England) 29:1072–1075. https://doi.org/10.1093/bioinformatics/btt086

Huerta-Cepas J, Forslund K, Coelho LP, Szklarczyk D, Jensen LJ, von Mering C, Bork P (2017) Fast genome-wide functional annotation through orthology assignment by eggNOG-Mapper. Mol Biol and Evol 34:2115–2122. https://doi.org/10.1093/molbev/msx148

Johnstone TC, Nolan EM (2015) Beyond iron: non-classical biological functions of bacterial siderophores. Dalton Trans 44:6320–6339. https://doi.org/10.1039/c4dt03559c

Kanehisa MGS, Goto S (2000) KEGG: Kyoto Encyclopedia of Genes and Genomes Nucleic acids research. Nucleic Acids Res 28:27–30. https://doi.org/10.1093/nar/28.1.27

Khilyas IV et al (2019) Microbial diversity and mineral composition of weathered serpentine rock of the Khalilovsky massif. PLoS ONE 14:e0225929. https://doi.org/10.1371/journal.pone.0225929

LeBlanc JC, Gonçalves ER, Mohn WW (2008) Global response to desiccation stress in the soil Actinomycete *Rhodococcus jostii* RHA1. Appl Environ Microbiol 74:2627. https://doi.org/10.1128/AEM.02711-07

Leon MJ, Hoffmann T, Sanchez-Porro C, Heider J, Ventosa A, Bremer E (2018) Compatible solute synthesis and import by the moderate halophile *Spiribacter salinus*: physiology and genomics. Front Microbiol 9:108. https://doi.org/10.3389/fmicb.2018.00108

Ljungh A, Hjerten S, Wadstrom T (1985) High surface hydrophobicity of autoaggregating *Staphylococcus aureus* strains isolated from human infections studied with the salt aggregation test. Infect Immun 47:522–526

Meier-Kolthoff JP, Auch AF, Klenk HP, Goker M (2013) Genome sequence-based species delimitation with confidence intervals and improved distance functions. BMC Bioinformat 14:60. https://doi.org/10.1186/1471-2105-14-60

Miranda-CasoLuengo R, Prescott JF, Vázquez-Boland JA, Meijer WG (2008) The intracellular pathogen *Rhodococcus equi* produces a catecholate siderophore required for saprophytic growth. J Bacteriol 190:1631–1637. https://doi.org/10.1128/jb.01570-07

Page AJ et al (2015) Roary: rapid large-scale prokaryote pan genome analysis. Bioinformatics 31:3691–3693. https://doi.org/10.1093/bioinformatics/btv421

Pevzner PA, Tang H, Waterman MS (2001) An Eulerian path approach to DNA fragment assembly. PNAS USA 98:9748–9753. https://doi.org/10.1073/pnas.171285098

Potts M (1994) Desiccation tolerance of prokaryotes. Microbiol Rev 58:755–805

Price MN, Dehal PS, Arkin AP (2010) FastTree 2 – Approximately maximum-likelihood trees for large alignments. PLoS ONE 5:e9490. https://doi.org/10.1371/journal.pone.0009490

Saha M, Sarkar S, Sarkar B, Sharma BK, Bhattacharjee S, Tribedi P (2016) Microbial siderophores and their potential applications: a review. Environ Sci Pollut Res Int 23:3984–3999. https://doi.org/10.1007/s11356-015-4294-0

Sangal V, Goodfellow M, Jones AL, Seviour RJ, Sutcliffe IC (2019) Refined systematics of the genus *Rhodococcus* based on whole genome analyses. In: Alvarez HM (ed) Biology of *Rhodococcus*. Springer, Cham

Shimodaira H, Hasegawa M (1999) Multiple comparisons of log-likelihoods with applications to phylogenetic inference. Mol Biol Evol 16:1114–1114. https://doi.org/10.1093/oxfordjournals.molbev.a026201

Sitto F, Battistuzzi FU (2019) Estimating pangenomes with roary molecular biology and evolution. Mole Biol 37:933–939. https://doi.org/10.1093/molbev/msz284

Stamatakis A (2014) RAxML version 8: a tool for phylogenetic analysis and post-analysis of large phylogenies. Bioinformatics (Oxford, England) 30:1312–1313. https://doi.org/10.1093/bioinformatics/btu033

Švec P et al (4446T) Classification of strain CCM 4446T as *Rhodococcus degradans* sp Nov. Int J Syst Evol Microbiol 65:4381–4387. https://doi.org/10.1099/ijsem.0.000584

Tancsics A et al (2014) Sequence analysis of 16S rRNA, *gyr*B and *cat*A genes and DNA-DNA hybridization reveal that *Rhodococcus jialingiae* is a later synonym of *Rhodococcus qingshengii*. Int J Syst Evol Microbiol 64:298–301. https://doi.org/10.1099/ijs.0.059097-0

Tatusova T et al (2016) NCBI prokaryotic genome annotation pipeline. Nucleic Acids Res 44:6614–6624. https://doi.org/10.1093/nar/gkw569

Xu JL, He J, Wang ZC, Wang K, Li WJ, Tang SK, Li SP (2007) *Rhodococcus qingshengii* sp. nov, a carbendazim-degrading bacterium. Int J Syst Evol Microbiol 57:2754–2757. https://doi.org/10.1099/ijs.0.65095-0

Zhou Y, Liang Y, Lynch KH, Dennis JJ, Wishart DS (2011) PHAST: a fast phage search tool. Nucleic Acids Res 39:W347–W352. https://doi.org/10.1093/nar/gkr485